



Tuning Functional Amyloid Formation Through Disulfide Engineering

Anthony Balistreri, Ethan Kahana, Soorya Janakiraman and Matthew R. Chapman*

Department of Molecular, Cellular and Developmental Biology, University of Michigan, Ann Arbor, MI, United States

OPEN ACCESS

Edited by:

Salvador Ventura,
Autonomous University of Barcelona,
Spain

Reviewed by:

Jan-Ulrik Dahl,
Illinois State University, United States
Alberto A. Iglesias,
National University of Littoral,
Argentina

*Correspondence:

Matthew R. Chapman
chapmanm@umich.edu

Specialty section:

This article was submitted to
Microbial Physiology and Metabolism,
a section of the journal
Frontiers in Microbiology

Received: 20 February 2020

Accepted: 20 April 2020

Published: 26 May 2020

Citation:

Balistreri A, Kahana E,
Janakiraman S and Chapman MR
(2020) Tuning Functional Amyloid
Formation Through Disulfide
Engineering. *Front. Microbiol.* 11:944.
doi: 10.3389/fmicb.2020.00944

Many organisms produce “functional” amyloid fibers, which are stable protein polymers that serve many roles in cellular biology. Certain Enterobacteriaceae assemble functional amyloid fibers called curli that are the main protein component of the biofilm extracellular matrix. CsgA is the major protein subunit of curli and will rapidly adopt the polymeric amyloid conformation *in vitro*. The rapid and irreversible nature of CsgA amyloid formation makes it challenging to study *in vitro*. Here, we engineered CsgA so that amyloid formation could be tuned to the redox state of the protein. A double cysteine variant of CsgA called CsgA_{CC} was created and characterized for its ability to form amyloid. When kept under oxidizing conditions, CsgA_{CC} did not adopt a β -sheet rich structure or form detectable amyloid-like aggregates. Oxidized CsgA_{CC} remained in a soluble, non-amyloid state for at least 90 days. The addition of reducing agents to CsgA_{CC} resulted in amyloid formation within hours. The amyloid fibers formed by CsgA_{CC} were indistinguishable from the fibers made by CsgA WT. When measured by thioflavin T fluorescence the amyloid formation by CsgA_{CC} in the reduced form displayed the same lag, fast, and plateau phases as CsgA WT. Amyloid formation by CsgA_{CC} could be halted by the addition of oxidizing agents. Therefore, CsgA_{CC} serves as a proof-of-concept for capitalizing on the convertible nature of disulfide bonds to control the aggregation of amyloidogenic proteins.

Keywords: disulfide engineering, functional amyloid, CsgA, curli, protein engineering

INTRODUCTION

Amyloids are fibril aggregates of proteins which have misfolded to form a characteristic cross β -sheet secondary structure (Chiti and Dobson, 2006). The fibers deposit in cells in dense bodies known as plaques and are implicated in many well-known neurodegenerative diseases including Alzheimer, Parkinson, and Huntington Disease (Chiti and Dobson, 2017). For this reason, the nature of amyloids and how they form is an active area of research. Though the disease causing amyloids are composed of misfolded proteins, there are now many examples of “functional amyloids” that organisms create for a predetermined purpose (Chapman et al., 2002; Otzen, 2010). These fibers are composed of proteins that adopt the amyloid fold not by misfolding, rather they do so intentionally and efficiently (Deshmukh et al., 2018). Functional amyloids provide researchers with well-defined and adaptable models for studying the basic tenets of amyloid formation.

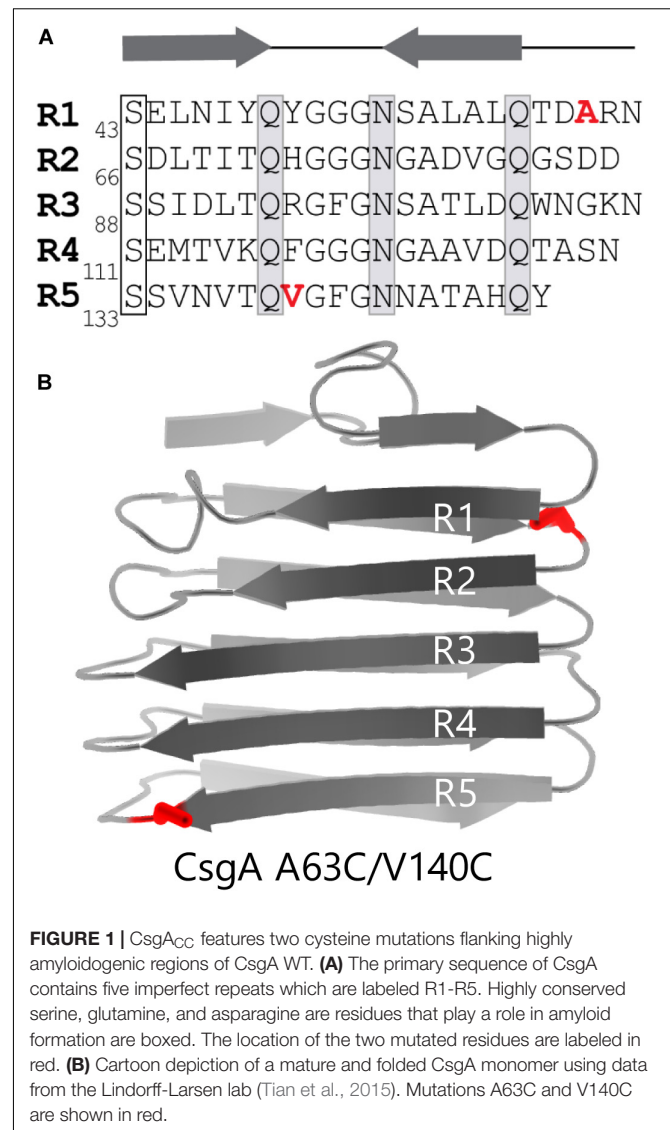
Curli are functional amyloids produced by *Escherichia coli* and other Enterobacteriaceae (Dueholm et al., 2012). Curli amyloids are the main proteinaceous component of the biofilm extracellular matrix (Chapman et al., 2002; Reichhardt and Cegelski, 2014). The major protein subunit of curli, called CsgA, is secreted in a monomeric, unstructured state (Wang et al., 2007).

CsgA undergoes self-assembly into curli fibers on the cell surface with the help of several auxiliary proteins belonging to the *csg* operon (Chapman et al., 2002; Robinson et al., 2006; Hammer et al., 2007; Wang et al., 2008; Nenninger et al., 2009, 2011; Evans et al., 2015; Jain and Chapman, 2019). Purified CsgA readily forms amyloid fibers and there are several methods to monitor *in vitro* amyloid aggregation (Wang et al., 2007; Evans et al., 2018). However, these techniques require handling protein samples which are in a constant state of aggregation (Evans et al., 2018).

To minimize CsgA aggregation into amyloid during purification, the current methodology relies on chemical denaturants (8M guanidinium hydrochloride) (Zhou et al., 2013). Though this protocol provides useable amounts of purified CsgA, there are still several purification steps that need to take place under non-denaturing conditions. During the final size exclusion and buffer exchange steps there is an unavoidable loss of soluble CsgA which is tolerated in exchange for speediness.

Here, we employ a different strategy to restrict amyloid formation. CsgA is an intrinsically disordered protein that transitions into a β -sheet rich conformation upon forming amyloid fibers (Wang et al., 2007). Therefore, a potential strategy for controlling aggregation is targeting this transition. Disulfide bonds are tertiary structural components of many natively folded proteins that aid in protein folding and provide stability (Anfinsen and Scheraga, 1975). They are also by nature convertible; they can be broken and reformed based on the redox state of the environment (Gilbert, 1995). By engineering two cysteine residues into its sequence, we can provide CsgA the option to form an intramolecular disulfide bond under the right conditions. Previous work has shown disulfide engineering can be used to stabilize the native fold state of a protein (Matsumurat et al., 1989; Dombkowski et al., 2014; Schmidt et al., 2015; Liu et al., 2016). Recently, other groups have used this technique to modulate amyloid formation of human amyloid proteins (Hoyer et al., 2008; Carija et al., 2019). In this study we harness disulfide engineering as a method for stabilizing the non-native fold state of a protein with the intention of triggering protein folding.

We created a double cysteine variant of CsgA called CsgA_{CC} with the goal of making CsgA amyloid formation tunable to its redox state. CsgA contains five imperfect repeat sequences (R1-R5) corresponding to five β -strands that exist in the final folded protein (Figure 1A; Wang et al., 2007). β -strands R1 and R5 are critical to the ability of CsgA to form amyloid (Wang et al., 2008). We hypothesized that the presence of an unnatural disulfide linkage near R1 and R5 would hinder CsgA from forming the secondary structure required for amyloid formation. In order to allow amyloid formation to eventually occur, regions of the sequence essential to proper folding needed to remain undisturbed. Therefore, the β -turn regions that flank R1 and R5 offered an amenable target region. The sequence of CsgA does not contain any native cysteine residues (Barnhart and Chapman, 2006). We decided to replace two residues of similar size and properties to cysteine in the regions of interest. Alanine-63 and valine-140 fulfilled the criteria and were replaced with cysteine residues (Figure 1B). As we hypothesized, we found that the ability of CsgA_{CC} to form amyloid could be stimulated



by the addition of a reducing agent, and that when kept in an oxidized form, CsgA_{CC} remained in a soluble and non-amyloid conformation.

MATERIALS AND METHODS

Bacterial Growth

All overnight cultures were grown in sterilized LB (Fisher Scientific) media supplemented with 100 μ g/mL ampicillin or 50 μ g/mL of kanamycin at 37°C with shaking at 220 rpm. When necessary, LB agar plates were supplemented with ampicillin 100 μ g/mL or kanamycin 50 μ g/mL.

Strains and Plasmids

A full list of strains, plasmids, and primers can be found in **Supplementary Tables S1, S2**. Site directed mutagenesis was performed on pre-existing plasmids

using the Agilent QuikChange II XL kit. Primers were designed by Agilent QuikChange Primer Design (<https://www.agilent.com/store/primerDesignProgram.jsp>) and synthesized by IDT (<https://www.idtdna.com>). Mutagenized plasmids were constructed in the MC1061 cell background. Mutations were confirmed using Sanger sequencing done at the UM Biomedical Research Core (<https://brcf.medicine.umich.edu/>). Plasmids were purified using Promega PureYield™ Plasmid Miniprep System. Miniprep plasmids were transformed into an expression strain (NEB3016), curli-competent strain (MC4100), or a curli-incompetent MC4100 variant strain that lacks *csgA* (LSR10).

Protein Purification

Recombinant CsgA and its variants were purified as described previously (Evans et al., 2018). An overnight liquid culture was prepared by inoculating 25 mL of LB media supplemented with 25 μ L of 100 mg/mL Ampicillin. The culture was grown up overnight in a shaking incubator at 37°C and 220 rpm. The following day two solutions containing 750 mL of LB media and 0.75 mL of 100 mg/mL Ampicillin were inoculated with a 1% inoculum of the overnight liquid culture. The culture was grown up in a shaking incubator at 37°C and 220 rpm until OD₆₀₀ = 0.8–0.9 was reached. Protein expression was induced by adding 375 μ L of 1M IPTG and continue to incubate for 1 h. Induced cells were spun down by centrifugation at 4,000 rpm for 20 min at 4°C and supernatant was discarded. Cell pellets representing 250 mL of culture volume were placed into 50 mL Falcon tube for storage and frozen at –80°C. A frozen cell pellet was retrieved from storage and resuspended in 25 mL of Lysis buffer (8 M guanidinium hydrochloride, 50 mM KPi, pH 7.3) and incubated at room temperature for 1 h on a rocking shaker. The cellular debris was spun down at 10,000 \times g for 20 min and the soluble fraction was collected. The soluble fraction was sonicated 3 \times 20 s using a probe sonicator. The sonicated mixture was incubated with 0.8 mL of HIS-Select® HF Nickel Affinity Gel (Sigma) and mixed at room temperature for 1 h. The mixture was loaded into a disposable 5 mL polypropylene column containing a fritted glass filter and the flow through was discarded. The column was washed with 10 mL of 50 mM KPi, pH 7.3 and 3 mL of wash buffer (12.5 mM imidazole in 50 mM KPi, pH 7.3), discarding the eluent. 5 mL of elution buffer (125 mM imidazole in 50 mM KPi, pH 7.3) was added to the column and incubated for 5 min at room temperature. The first 0.5 mL of eluent was set aside and the next 1 mL elution fraction was collected. A 2 mL Zeba™ Spin Desalting Column (Pierce) was rinsed twice with 50 mM KPi, pH 7.3 by centrifuging at 1,000 rpm for 2.5 min. The elution fraction was loaded into the column and spun down into a clean 15 mL Falcon tube. The flow through was moved to a cooled Amicon® 30K cut-off filter column and centrifuge at 7,000 \times g for 10 min to result in the final solution containing purified protein. After purification, CsgA proteins were stored in 50 mM KPi, pH 7.3 buffer at 4°C unless stated otherwise. Size exclusion chromatography was performed on CsgA_{ACC} samples essentially as previously described (Evans et al., 2018). Ni-NTA elution fractions were concentrated using a cooled Amicon® 3K cut-off Spin Column centrifuged

at 7,000 rcf for 10 min at 4°C until the total volume was 2 mL. When the desired volume was reached, the retentate was moved to MilliporeSigma™ Ultrafree™-MC Centrifugal Filters and centrifuged to remove any particulates. The filtered samples underwent gel filtration using a GE Superdex 75 10/300 GL column attached to an Äkta pure protein purification system and the elution buffer was 50 mM KPi, pH 7.3. FLPC elution fractions were assayed for protein concentration using A220. Samples corresponding to elution peaks were analyzed using reducing (with added β -mercaptoethanol) and non-reducing (without β -mercaptoethanol) SDS-PAGE. CsgC was purified as described previously (Salgado et al., 2011).

Circular Dichroism (CD)

200 μ L of purified protein samples of CsgA WT and CsgA_{ACC} were added directly into a quartz cell with a 1 cm path. CD spectra were obtained using a Jasco J-1500 CD Spectrometer by scanning from 190 to 260 nm at 25°C. Where indicated, tris(2-carboxyethyl)phosphine (TCEP) was added from a stock solution (200 mM TCEP in MQ water, pH = 7.7) to a final concentration of 8 mM. The spectrum of the appropriate buffer-only control was subtracted from each sample as a baseline. **Figure 3A** includes three purification batches Batch 1 (44 μ M) Batch 2 (22 μ M) and Batch 3 (16 μ M) stored at 4°C in 50 mM KPi, pH 7.3. For the spectra shown in **Figure 3B**, 20 μ M CsgA WT was stored at room temperature in 20 mM KPi, pH 7.3 that contained 25 μ M PMSF. Finally, **Figure 3C** includes 20 μ M CsgA_{ACC} was that stored at 4°C in 50 mM KPi, pH 7.3.

Denaturing Gel Electrophoresis and Western Blot

Purified protein samples were diluted in 2X SDS loading buffer (1 mL 1.25 M Tris base pH 6.8, 1 mL β -mercaptoethanol, 200 μ L 1% bromophenol blue, 2 mL glycerol, 6 mL 10% SDS and 10 mL water) with or without β -mercaptoethanol and run on a 15% SDS PAGE gel (Evans et al., 2018). The gels were microwaved in 30 mL of Coomassie blue dye for 20 s and destained with MQ water overnight to visualize protein bands. Western Blot were performed as previously described using the wet transfer method (Evans et al., 2018). Briefly, blots were probed with a primary antibody against CsgA (1:12,000). Secondary antibodies against rabbit IgG and conjugated with IRDye 800CW were used to image the blots in a LI-COR Odyssey® Fc.

Gel Solubility Assay

Freshly purified samples of CsgA WT and CsgA_{ACC} were transferred to a microcentrifuge tube, diluted to 20 μ M in 50 mM KPi pH = 7.3, and allowed to incubate at room temperature. Where indicated, tris(2-carboxyethyl)phosphine (TCEP) was added from a stock solution (200 mM TCEP in MQ water, pH = 7.7) to a final concentration of 8 mM. Gel samples were removed at 0, 24, and 48 h after purification. The gel samples were diluted in 4X SDS loading buffer and run on a 15% SDS PAGE gel (Evans et al., 2018). The gels were stained with Coomassie blue dye. Destained gels were scanned using the 700 nm channel of a LI-COR Odyssey® Fc. Band intensity was quantified using ImageJ

(<https://imagej.nih.gov/ij/>) and normalized to the CsgA WT time 0 no TCEP added condition.

Transmission Electron Microscopy

TEM images were produced as previously described (Jain et al., 2017). Briefly, 5 μ L of purified protein samples were spotted onto a formvar/carbon 200 mesh copper grid. After a 5 min incubation, grids were spotted with 5 μ L of DI water followed by 5 μ L of 2% uranyl acetate to provide micrograph image contrast. Grids were imaged using a Jeol JEM 1400plus Transmission Electron Microscope.

Thioflavin T Binding Assay

Th-T assays were performed as previously described (Zhou et al., 2012). Briefly, freshly purified CsgA was diluted with 50 mM KPi, pH 7.3 to 20 μ M and combined with 20 μ M of the amyloid-specific dye thioflavin-T (Th-T). Selected samples were reduced with the addition of tris(2-carboxyethyl)phosphine (TCEP) from a stock solution (200 mM TCEP in MQ water, pH = 7.7). Amyloid formation was monitored by measuring an increase in Th-T fluorescence at 495 nM (450 nM excitation). Assays were performed in triplicate at microscale within 96-well plates and measured with Tecan infinite[®] Pro M200 or infinite[®] Nano⁺ F200 microplate readers. In **Figures 4–6, 8** the data were normalized by the largest value of the CsgA WT condition performed at the same time in each experiment. When specified, Th-T assays included the following additions: FN075 diluted from a 50 mM stock solution (DMSO) sourced from the Almqvist Lab (Department of Chemistry, University of Umeå, Sweden), CsgC purified and diluted from a stock solution (phosphate buffer), CsgA WT fibers purified previously and sonicated directly before addition, and hydrogen peroxide.

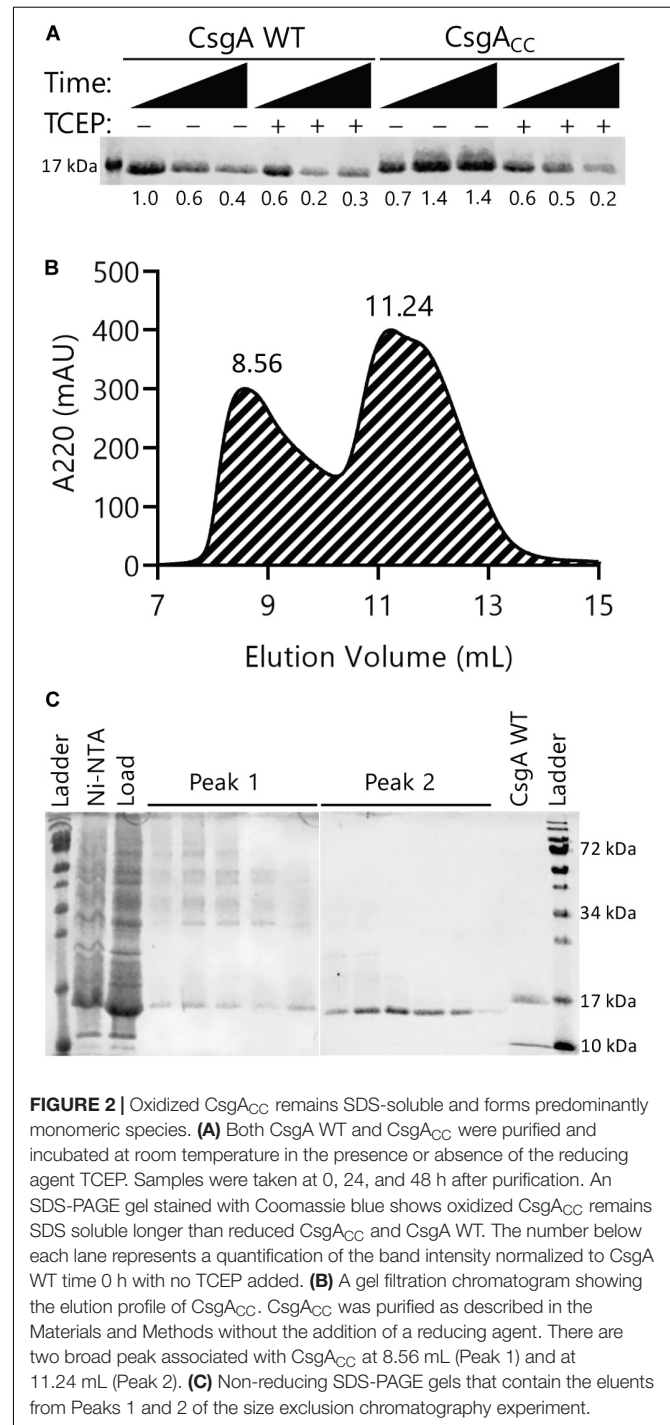
Complementation Assay

Congo Red binding assays were performed as previously described (Evans et al., 2018). Overnight liquid cultures were normalized to OD = 1 and a 200 μ L aliquot was spun down at 13 k rpm and the supernatant was decanted. The cell pellets were washed by resuspending, pelleting, and decanting the cells in YESCA media (1 g yeast extract, 10 g casamino acids and 20 g agar in 1 L water). After the third wash, the cells were resuspended in 200 μ L YESCA and 4 μ L was spotted onto a YESCA agar plate supplemented with 50 μ g/mL Congo Red. The plates were incubated at 26°C for 48 h to allow for curli formation. After that time plates were photographed to generate the images used in **Figure 7A**.

RESULTS

Immediately after purification CsgA is intrinsically disordered with a random coil secondary structure. Within hours, CsgA aggregates into stable, β -rich amyloid fibers (Wang et al., 2007). To control amyloid aggregation by CsgA we hypothesized that strategically-placed cysteine residues would allow the generation of a CsgA molecule that could be locked in a non-amyloid state

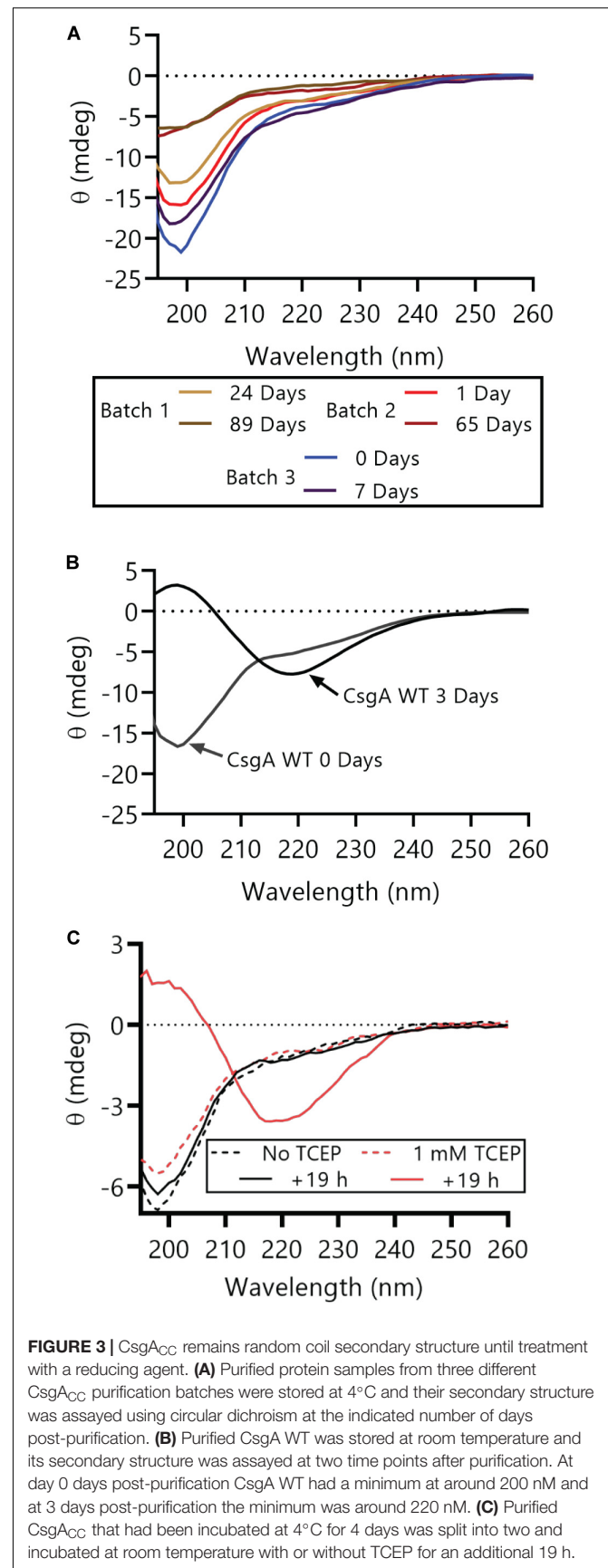
(**Figure 1**). The wildtype sequence of *E. coli* CsgA does not contain native cysteine residues (**Figure 1A**). Cysteine residues were engineered into CsgA at positions alanine-63 and valine-140 using site-directed mutagenesis. The resulting protein, called CsgA_{CC}, was purified and characterized. From this point forward native CsgA will be referred to as CsgA WT and CsgA that contains cysteine residues at positions 63 and 140 will be referred to as CsgA_{CC}.

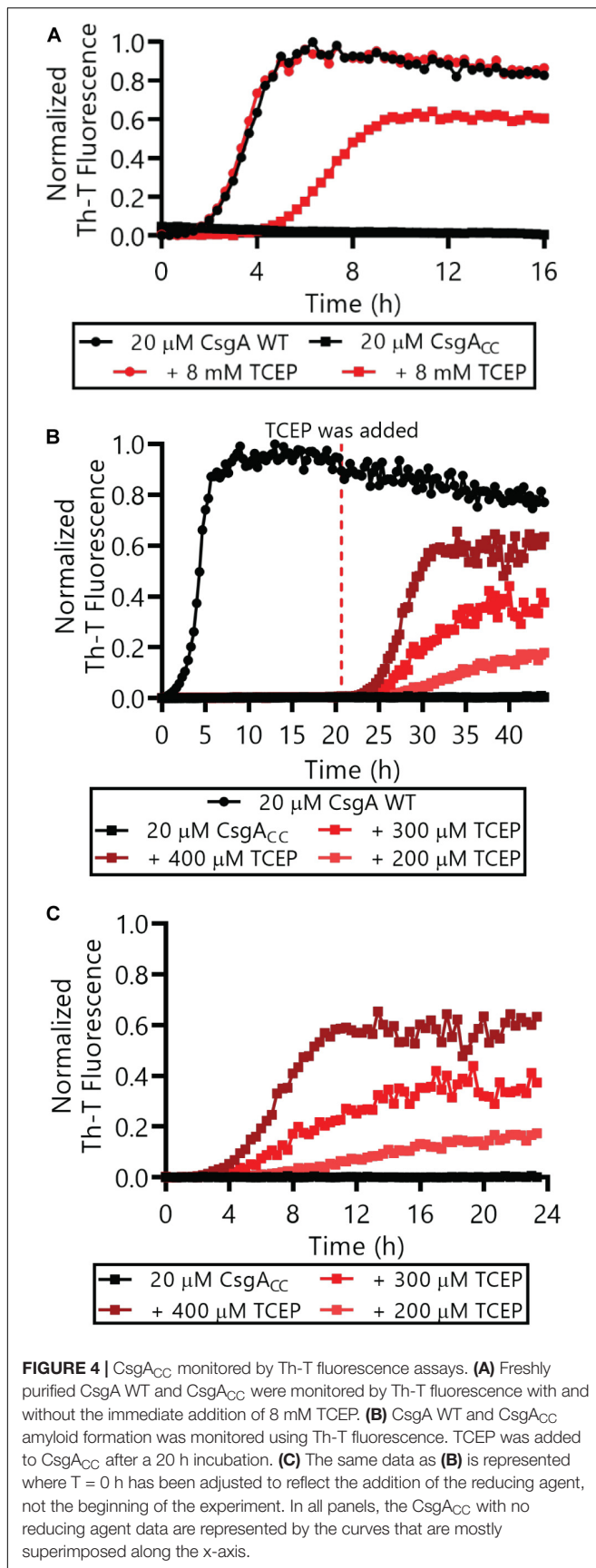


We found that freshly purified and oxidized CsgA_{CC} remained SDS soluble for at least 48 h (Figure 2A). For comparison, both CsgA WT and CsgA_{CC} that was incubated with the reducing agent TCEP displayed a marked decrease in SDS solubility over a 48 h period (Figure 2A). Because CsgA_{CC} remained soluble, size exclusion chromatography could be used to determine what types of protein species were present after purification. Freshly purified CsgA_{CC} was subjected to gel filtration and the protein eluted off the column in two wide peaks at 8.56 (peak 1) and 11.24 mL (peak 2) elution volume (Figure 2B). Analytical gel filtration chromatography can normally be used to provide an estimate of an analyte's size by comparing column retention times with known globular proteins in a standard curve (Whitaker, 1963). However, because CsgA_{CC} remained unstructured, the globular proteins did not provide comparable retention profiles (Sambi et al., 2010). We therefore used non-reducing SDS-PAGE analysis to view what size protein species were in solution (Figure 2C). The second and larger peak corresponded to the monomeric species of CsgA_{CC} (Figure 2C). When samples from peak 1 of the gel filtration were analyzed by non-reducing SDS-PAGE, there were several slowly migrating bands (Figure 2C). When the same samples from peak 1 were analyzed by SDS-PAGE that included a reducing agent, β -mercaptoethanol, many of the high molecular weight bands disappeared, suggesting that CsgA_{CC} forms homo-oligomers that disassociate when reduced (Supplementary Figure S1). The monomeric species of CsgA_{CC} incubated under oxidized conditions ran faster on the SDS-PAGE gel than CsgA WT prepared in the same manner (Figure 2C). It is possible that in a non-reducing environment the intramolecular disulfide bond that holds CsgA_{CC} in a constrained conformation results in the faster migration of CsgA_{CC} relative to CsgA WT.

Oxidized CsgA_{CC} can remain in a non-aggregated and non-amyloid form for much longer than CsgA WT. As measured by circular dichroism (CD), CsgA_{CC} remained in a random coil conformation for at least 89 days when stored under oxidizing conditions at 4°C (Figure 3A). CsgA WT transitions from random coil to β -sheet rich in less than 3 days (Figure 3B). When TCEP was added to CsgA_{CC} after 4 days of incubation under oxidizing conditions, CsgA_{CC} transitioned from random coil to β -sheet rich secondary structure (Figure 3C). This suggested that the redox state of CsgA_{CC} is a critical determinant of its secondary structure.

The Thioflavin-T (Th-T) binding assay is the most widely used method for monitoring *in vitro* amyloid formation in real time (Nilsson, 2004). CsgA WT amyloid formation displays a characteristic sigmoidal curve during which Th-T fluorescence begins to increase after a 2–4 h lag phase (Wang et al., 2007). Importantly, CsgA_{CC} showed no detectable increase in Th-T fluorescence unless treated with a reducing agent, even after prolonged incubation at room temperature (Figure 4 and Supplementary Figures S2, S3). There was a dose-dependent response of CsgA_{CC} amyloid formation when TCEP was added in a range between 400 and 200 μ M (Figures 4B,C). In all experiments there was an observable decrease in overall fluorescence seen in CsgA_{CC} Th-T binding assays when compared to CsgA WT (Figures 4, 8). In order to verify that intramolecular disulfide bonds played a role in inhibiting CsgA_{CC}

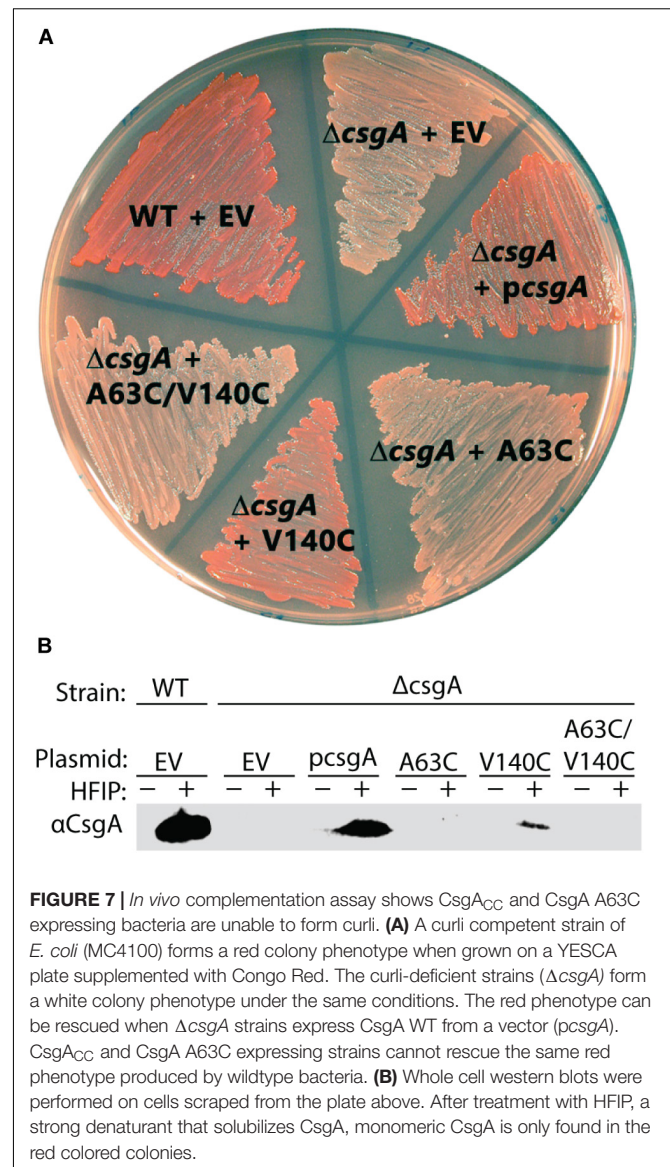
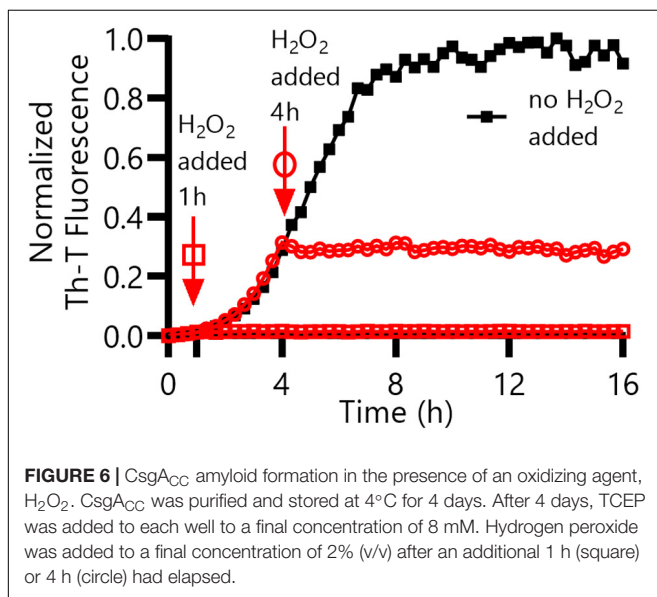
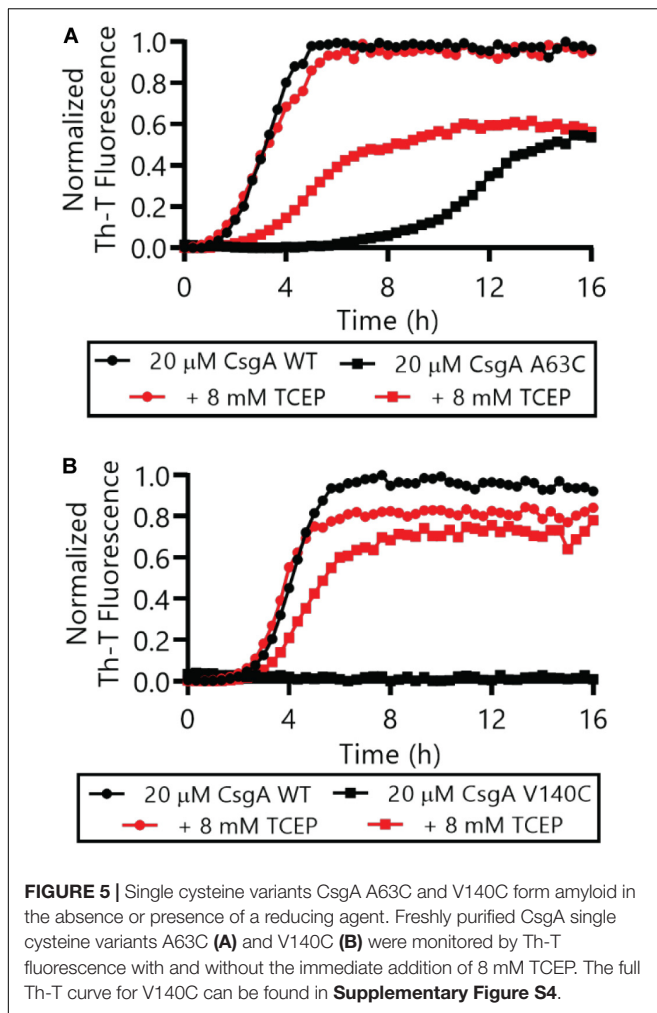




amyloid formation, we characterized the two single cysteine variants' ability to form amyloid. The introduction of a single cysteine mutation at either position 63 or 140 was only sufficient to slow down amyloid formation under oxidized conditions. A63C (**Figure 5A**) and V140C (**Figure 5B**) formed amyloid with and without the treatment of reducing agent, displaying an extended lag phase when compared to wildtype. Though V140C showed a lag phase that was much longer than A63C (**Supplementary Figure S4**). It should be noted that the addition of a reducing agent has no effect on the rate of CsgA WT amyloid formation (**Figure 5** and **Supplementary Figure S2B**). In an experiment where CsgA_{CC} amyloid formation had reached a fast growth phase, it could be prematurely stopped after the addition of an oxidizing agent like hydrogen peroxide (**Figure 6**). These experiments confirmed that CsgA_{CC} amyloid formation is susceptible to change given the redox state of its environment.

The ability of CsgA_{CC} to form amyloid *in vivo* was assessed. Curli-producing *E. coli* display a red colony phenotype when grown on a plate supplemented with the amyloid-binding dye Congo Red (Hammar et al., 1995; Evans et al., 2018). A Δ csgA mutant that can no longer produce curli forms white colonies on Congo Red indicator plates (Hammar et al., 1995; Evans et al., 2018). The red colony phenotype can be rescued in a Δ csgA strain when CsgA WT is supplied by a plasmid containing the csgA gene downstream of the natural promoter (Hammar et al., 1995; Evans et al., 2018; **Figure 7A**). When Δ csgA strains were complemented with a plasmid encoding the variants CsgA A63C, CsgA V140C, and CsgA_{CC} the resulting colonies were white, red, and white, respectively (**Figure 7A**). Whole cell western blot analysis showed the strain producing V140C was the only strain to harbor protein recognized by a α CsgA antibody (**Figure 7B**). Therefore, cysteine residues at the 63rd position or at positions 63 and 140 are more disruptive to curli formation than a single cysteine residue in the valine-140 position. The combination of color phenotype and negative western blot results found in the A63C and CsgA_{CC} samples coincided with previously published work describing Δ csgG and Δ csgE mutants (Robinson et al., 2006; Nenninger et al., 2011). It is possible that CsgA A63C and CsgA_{CC} are confined to the periplasm and subjected to proteolytic degradation in the same manner as CsgA WT in Δ csgG and Δ csgE mutants (Robinson et al., 2006; Nenninger et al., 2011).

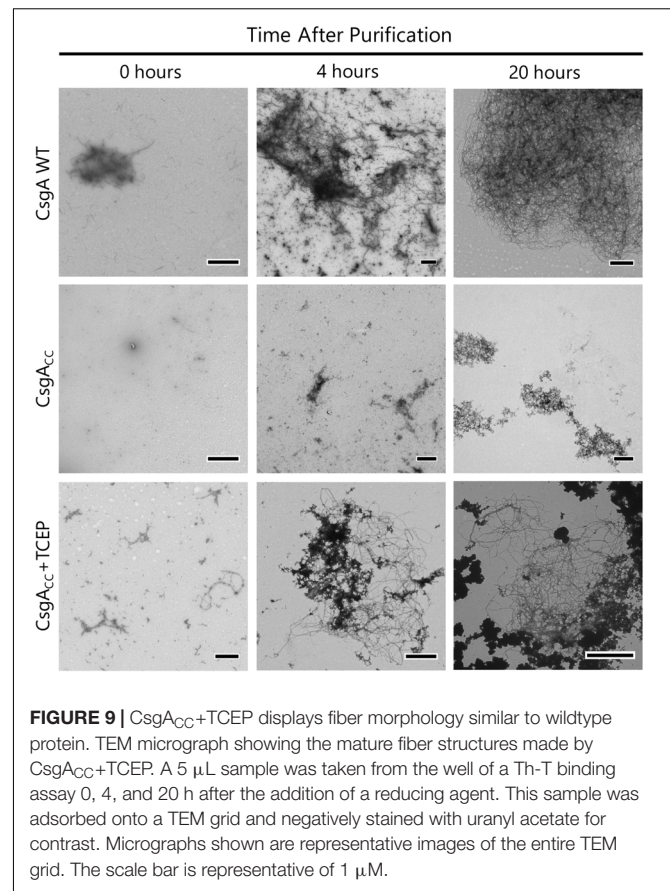
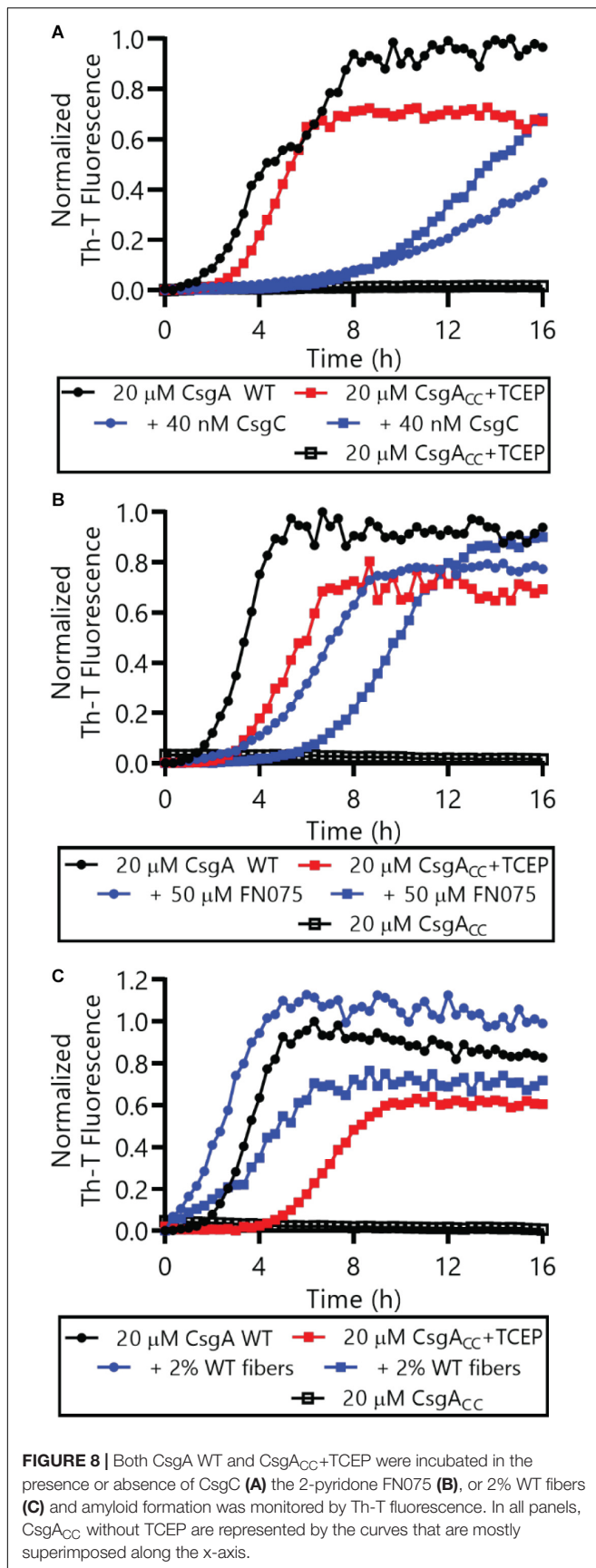
We also determined whether reduced CsgA_{CC}, or CsgA_{CC}+TCEP, interacted with certain proteins and small molecules in a similar manner to CsgA WT. Amyloid formation by CsgA WT is inhibited by the CsgC chaperone and also by a 2-pyridone called FN075 (Cegelski et al., 2009; Evans et al., 2015). We incubated CsgA WT and CsgA_{CC}+TCEP with inhibitory concentrations of FN075 and CsgC and monitored amyloid formation (**Figures 8A,B**). Both CsgA WT and CsgA_{CC}+TCEP amyloid formation were inhibited *in vitro* with similar efficiencies (**Figures 8A,B**). Conversely, amyloid formation can be sped up through a "seeding" effect when a small amount of preformed fibers are introduced to freshly purified CsgA WT (Wang et al., 2007). CsgA_{CC}+TCEP amyloid formation was similarly sped up when mixed with CsgA WT fibers (**Figure 8C**). Finally, CsgA_{CC} +TCEP formed fibril structures of identical morphology



with wildtype fibers as confirmed by transmission electron microscopy (Figure 9). Fibers could not be found in oxidized CsgA_{CC} samples (Figure 9). This line of evidence suggested that CsgA_{CC}, after being reduced, behaves similarly to CsgA WT *in vitro*.

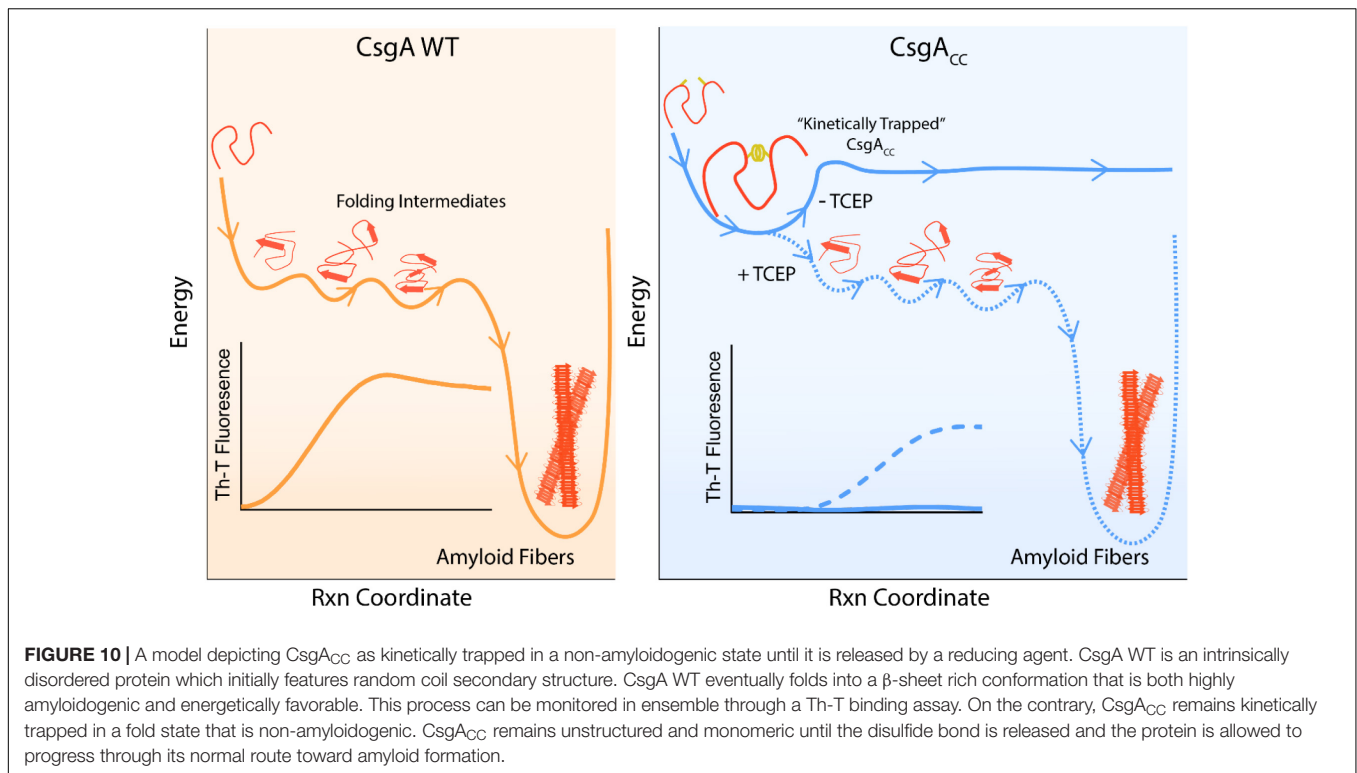
DISCUSSION

CsgA WT can transition from a mono dispersed, random coil structure to β -rich amyloid fibers within about 3 h (Wang et al., 2007). Indeed, the amyloid fiber conformation represents a very favorable energy minimum for amyloidogenic proteins (Eisenberg and Jucker, 2012). CsgA_{CC} incubated under oxidizing conditions remains in a random coil, non-amyloidogenic state for at least 88 days (Figure 3). The oxidized disulfide bond



“kinetically traps” CsgA_{CC} in a fold state of relatively high energy compared to the amyloid conformation into which each protein would naturally deposit (Figure 10). In a reducing environment, the transition of CsgA_{CC} into the amyloid conformation required no additional heat or chemical energy at all (Figure 3B). Moreover CsgA_{CC} exhibits a consistent Th-T lag phase of no shorter than 2–4 h after reduction (Figures 4, 8). Therefore, when CsgA_{CC} is “kinetically trapped” in an oxidized environment, it must be trapped in a way that prevents nucleus formation. The introduction of a nucleating species, such as sonicated fibers, to amyloid-competent proteins provides a dramatic decrease in an energy barrier leading to rapid amyloid formation (Gosal et al., 2005). However, providing oxidized CsgA_{CC} with preformed fibers did not spark amyloid formation (Supplementary Figure S5). CsgA_{CC} transitions from an amyloid-incompetent species to an amyloid-competent species only after the disulfide bond is reduced (Figure 10).

Here, we have shown CsgA_{CC} forms amyloid only when incubated in the presence of a reducing agent (Figures 4, 8), affording a method to tune CsgA_{CC} aggregation depending on its redox state. CsgA_{CC} amyloid formation is sensitive to reducing agent in a dose-dependent manner (Figure 4), thus providing control over when amyloid formation occurs. Because CsgA_{CC} can be kept in a non-amyloidogenic form it should allow for easier purification, handling, and storage of the protein.



CsgA_{CC} could lend itself to understanding the nucleation phase, which is currently poorly understood for functional amyloids like CsgA WT (Arosio et al., 2015). CsgA WT amyloid formation begins directly after purification (Wang et al., 2007; Zhou et al., 2013). By the time we start to monitor CsgA WT amyloid formation by Th-T fluorescence, aggregation and nuclei formation has already started (Sleutel et al., 2017). On the contrary, CsgA_{CC} amyloid formation can be started and stopped at any desired time by the addition of a reducing or oxidizing agent (Figure 6). The ability to halt amyloid formation at different points in the process could allow the characterization of amyloid fiber intermediates. Thus the earliest amyloid processes such as the transition of monomers to oligomers or the formation of nucleating species can be better resolved.

After the addition of an oxidizing agent to CsgA_{CC}+TCEP, there is no decrease in Th-T fluorescence observed, but instead the Th-T positive species that had formed seem to persist for at least 12 h (Figure 6), suggesting two things. First, during the Th-T growth phase there must be monomers in solution which are still susceptible to forming a disulfide bond that makes them amyloid-incompetent. Second, in a model of amyloid formation wherein the fiber end is in a state of equilibrium with free protein monomers, there would be a k_{on} and k_{off} that described the addition/subtraction of monomers to/from the fiber. If this were the case, then monomers that subtract from the fiber could become susceptible to oxidation. The excess of oxidizing agent would greatly shift the equilibrium in the direction of free, oxidized protein monomers and fibers would begin to unravel at the fiber ends. Because the curve in Figure 6 does not show a time-dependent decrease in Th-T fluorescence, it appears that

oxidized CsgA_{CC} amyloid fibers and their fiber ends are stable over at least 12 h.

CONCLUSION

In this study, we have shown the ability to tune aggregation of a functional amyloid protein by engineering a disulfide bond into CsgA from *E. coli*. CsgA_{CC} remains in a soluble, non-amyloidogenic state until the disulfide is reduced (Figures 2A, 4). Once reduced, amyloid formation can be manipulated depending on the redox state of the environment (Figure 6). CsgA_{CC} is a tool that makes studying amyloid formation easier and offers researchers extra time and control, two highly valuable resources. Purified CsgA_{CC} samples can now be prepared ahead of time, concentrated, and stored. This method of using disulfide engineering to control amyloid formation could be translated to other functional and human diseases-causing amyloids. Furthermore, the growing field of bio-inspired nanotechnology is capitalizing on the self-assembly of amyloid proteins. CsgA has been shown to have range of uses such as the passage of electric current, the extraction of rare earth metals, and many others (Nguyen et al., 2014; Seker et al., 2017; Tay et al., 2018). The work presented here will allow material scientists to use amyloid fibers to build systems of higher complexity than is currently possible.

DATA AVAILABILITY STATEMENT

The datasets generated for this study are available on request to the corresponding author.

AUTHOR CONTRIBUTIONS

AB and MC contributed to the conception and design of the study. AB, EK, and SJ performed the experiments. AB wrote the manuscript. AB and MC contributed to the editing and revising of the manuscript.

FUNDING

This work was supported by the National Institutes of Health grant nos. R01 GM118651 and R21 AI137535 to MC.

REFERENCES

- Anfinsen, C. B., and Scheraga, H. A. (1975). Experimental and theoretical aspects of protein folding. *Adv. Protein Chem.* 29, 205–300. doi: 10.1016/S0065-3233(08)60413-1
- Arosio, P., Knowles, T. P. J., and Linse, S. (2015). On the lag phase in amyloid fibril formation. *Phys. Chem. Chem. Phys.* 17, 7606–7618. doi: 10.1039/c4cp05563b
- Barnhart, M. M., and Chapman, M. R. (2006). Curli biogenesis and function. *Annu. Rev. Microbiol.* 60, 131–147. doi: 10.1146/annurev.micro.60.080805.142106
- Carija, A., Pinheiro, F., Pujols, J., Brás, I. C., Lázaro, D. F., Santambrogio, C., et al. (2019). Biasing the native α -synuclein conformational ensemble towards compact states abolishes aggregation and neurotoxicity. *Redox Biol.* 22:101135. doi: 10.1016/j.redox.2019.101135
- Cegelski, L., Pinkner, J. S., Hammer, N. D., Cusumano, C. K., Hung, C. S., Chorell, E., et al. (2009). Small-molecule inhibitors target *Escherichia coli* amyloid biogenesis and biofilm formation. *Nat. Chem. Biol.* 5, 913–919. doi: 10.1038/nchembio.242
- Chapman, M. R., Robinson, L. S., Pinkner, J. S., Roth, R., Heuser, J., Hammar, M., et al. (2002). Role of *Escherichia coli* curli operons in directing amyloid fiber formation. *Science* 295, 851–855. doi: 10.1126/science.1067484
- Chiti, F., and Dobson, C. M. (2006). Protein misfolding, functional amyloid, and human disease. *Annu. Rev. Biochem.* 75, 333–366. doi: 10.1146/annurev.biochem.75.101304.123901
- Chiti, F., and Dobson, C. M. (2017). Protein misfolding, amyloid formation, and human disease: a summary of progress over the last decade. *Annu. Rev. Biochem.* 86, 27–68. doi: 10.1146/annurev-biochem-061516-045115
- Deshmukh, M., Evans, M. L., and Chapman, M. R. (2018). Amyloid by design: intrinsic regulation of microbial amyloid assembly. *J. Mol. Biol.* 430, 3631–3641. doi: 10.1016/j.jmb.2018.07.007
- Dombkowski, A. A., Sultana, K. Z., and Craig, D. B. (2014). Protein disulfide engineering. *FEBS Lett.* 588, 206–212. doi: 10.1016/j.febslet.2013.11.024
- Dueholm, M. S., Albertsen, M., Otzen, D., and Nielsen, P. H. (2012). Curli functional amyloid systems are phylogenetically widespread and display large diversity in operon and protein structure. *PLoS One* 7:e51274. doi: 10.1371/journal.pone.0051274
- Eisenberg, D., and Jucker, M. (2012). The amyloid state of proteins in human diseases. *Cell* 148, 1188–1203. doi: 10.1016/j.cell.2012.02.022
- Evans, M. L., Chorell, E., Taylor, J. D., Åden, J., Göthesson, A., Li, F., et al. (2015). The bacterial curli system possesses a potent and selective inhibitor of amyloid formation. *Mol. Cell* 57, 445–455. doi: 10.1016/j.molcel.2014.12.025
- Evans, M. L., Gichana, E., Zhou, Y., and Chapman, M. R. (2018). “Bacterial amyloids,” in *Methods in Molecular Biology*, eds E. Sigurdsson, M. Calero, and M. Gasset (New York, NY: Humana Press Inc), 267–288. doi: 10.1007/978-1-4939-7816-8_17
- Gilbert, H. F. (1995). Thiol/disulfide exchange equilibria and disulfidebond stability. *Methods Enzymol.* 251, 8–28. doi: 10.1016/0076-6879(95)51107-5
- Gosal, W. S., Morten, I. J., Hewitt, E. W., Smith, D. A., Thomson, N. H., and Radford, S. E. (2005). Competing pathways determine fibril morphology in

ACKNOWLEDGMENTS

We would like to thank members of the Chapman lab and Alan Dombkowski for supportive conversations about the topic. Members of the Zhang and Brooks lab at University of Michigan provided helpful insight in the initiation of the concept.

SUPPLEMENTARY MATERIAL

The Supplementary Material for this article can be found online at: <https://www.frontiersin.org/articles/10.3389/fmicb.2020.00944/full#supplementary-material>

- the self-assembly of β 2-microglobulin into amyloid. *J. Mol. Biol.* 351, 850–864. doi: 10.1016/j.jmb.2005.06.040
- Hammar, M., Arnqvist, A., Bian, Z., Olsén, A., and Normark, S. (1995). Expression of two csg operons is required for production of fibronectin- and Congo red-binding curli polymers in *Escherichia coli* K-12. *Mol. Microbiol.* 18, 661–670. doi: 10.1111/j.1365-2958.1995.mmi_18040661.x
- Hammer, N. D., Schmidt, J. C., and Chapman, M. R. (2007). The curli nucleator protein, CsgB, contains an amyloidogenic domain that directs CsgA polymerization. *Proc. Natl. Acad. Sci. U.S.A.* 104, 12494–12499. doi: 10.1073/pnas.0703310104
- Hoyer, W., Grönwall, C., Jonsson, A., Ståhl, S., and Härd, T. (2008). Stabilization of a β -hairpin in monomeric Alzheimer’s amyloid- β peptide inhibits amyloid formation. *Chemtracts* 20, 499–500. doi: 10.1073/pnas.0711731105
- Jain, N., Aden, J., Nagamatsu, K., Evans, M. L., Li, X., McMichael, B., et al. (2017). Inhibition of curli assembly and *Escherichia coli* biofilm formation by the human systemic amyloid precursor transthyretin. *Proc. Natl. Acad. Sci. U.S.A.* 114, 12184–12189. doi: 10.1073/pnas.1708805114
- Jain, N., and Chapman, M. R. (2019). Bacterial functional amyloids: order from disorder. *Biochim. Biophys. Acta Proteins Proteom.* 1867, 954–960. doi: 10.1016/j.bbapap.2019.05.010
- Liu, T., Wang, Y., Luo, X., Li, J., Reed, S. A., Xiao, H., et al. (2016). Enhancing protein stability with extended disulfide bonds. *Proc. Natl. Acad. Sci. U.S.A.* 113, 5910–5915. doi: 10.1073/pnas.1605363113
- Matsumurat, M., Beckett, W. J., Levitr, M., and Matthewstl, B. W. (1989). Stabilization of phage T4 lysozyme by engineered disulfide bonds (thermostability/lysozyme/protein structure). *Biochemistry* 86, 6562–6566. doi: 10.1073/pnas.86.17.6562
- Neeninger, A. A., Robinson, L. S., Hammer, N. D., Epstein, E. A., Badtke, M. P., Hultgren, S. J., et al. (2011). CsgE is a curli secretion specificity factor that prevents amyloid fibre aggregation. *Mol. Microbiol.* 81, 486–499. doi: 10.1111/j.1365-2958.2011.07706.x
- Neeninger, A. A., Robinson, L. S., and Hultgren, S. J. (2009). Localized and efficient curli nucleation requires the chaperone-like amyloid assembly protein CsgF. *Proc. Natl. Acad. Sci. U.S.A.* 106, 900–905. doi: 10.1073/pnas.0812143106
- Nguyen, P. Q., Botyanszki, Z., Tay, P. K. R., and Joshi, N. S. (2014). Programmable biofilm-based materials from engineered curli nanofibres. *Nat. Commun.* 5:5945. doi: 10.1038/ncomms5945
- Nilsson, M. R. (2004). Techniques to study amyloid fibril formation in vitro. *Methods* 34, 151–160. doi: 10.1016/j.ymeth.2004.03.012
- Otzen, D. (2010). Functional amyloid: turning swords into plowshares. *Prion* 4, 256–264. doi: 10.4161/PRI.4.4.13676
- Reichhardt, C., and Cegelski, L. (2014). Solid-state NMR for bacterial biofilms. *Mol. Phys.* 112, 887–894. doi: 10.1080/00268976.2013.837983
- Robinson, L. S., Ashman, E. M., Hultgren, S. J., and Chapman, M. R. (2006). Secretion of curli fibre subunits is mediated by the outer membrane-localized CsgG protein. *Mol. Microbiol.* 59, 870–881. doi: 10.1111/j.1365-2958.2005.04997.x
- Salgado, P. S., Taylor, J. D., Cota, E., and Matthews, S. J. (2011). Extending the usability of the phasing power of diselenide bonds: SeCys SAD phasing of CsgC

- using a non-auxotrophic strain. *Acta Crystallogr. D. Biol. Crystallogr.* 67, 8–13. doi: 10.1107/S0907444910042022
- Sambi, I., Gatti-Lafranconi, P., Longhi, S., and Lotti, M. (2010). How disorder influences order and vice versa - mutual effects in fusion proteins containing an intrinsically disordered and a globular protein. *FEBS J.* 277, 4438–4451. doi: 10.1111/j.1742-4658.2010.07825.x
- Schmidt, S., Genz, M., Balke, K., and Bornscheuer, U. T. (2015). The effect of disulfide bond introduction and related Cys/Ser mutations on the stability of a cyclohexanone monooxygenase. *J. Biotechnol.* 214, 199–211. doi: 10.1016/J.JBIOTECH.2015.09.026
- Seker, U. O. S., Chen, A. Y., Citorik, R. J., and Lu, T. K. (2017). Synthetic biogenesis of bacterial amyloid nanomaterials with tunable inorganic-organic interfaces and electrical conductivity. *ACS Synth. Biol.* 6, 266–275. doi: 10.1021/acssynbio.6b00166
- Sleutel, M., Van den Broeck, I., Van Gerven, N., Feuillie, C., Jonckheere, W., Valotteau, C., et al. (2017). Nucleation and growth of a bacterial functional amyloid at single-fiber resolution. *Nat. Chem. Biol.* 13, 902–908. doi: 10.1038/nchembio.2413
- Tay, P. K. R., Manjula-Basavanna, A., and Joshi, N. S. (2018). Repurposing bacterial extracellular matrix for selective and differential abstraction of rare earth elements. *Green Chem.* 20, 3512–3520. doi: 10.1039/c8gc01355a
- Tian, P., Boomsma, W., Wang, Y., Otzen, D. E., Jensen, M. H., and Lindorff-Larsen, K. (2015). Structure of a functional amyloid protein subunit computed using sequence variation. *J. Am. Chem. Soc.* 137, 22–25. doi: 10.1021/ja5093634
- Wang, X., Hammer, N. D., and Chapman, M. R. (2008). The molecular basis of functional bacterial amyloid polymerization and nucleation. *J. Biol. Chem.* 283, 21530–21539. doi: 10.1074/jbc.M800466200
- Wang, X., Smith, D. R., Jones, J. W., and Chapman, M. R. (2007). In vitro polymerization of a functional *Escherichia coli* amyloid protein. *J. Biol. Chem.* 282, 3713–3719. doi: 10.1074/jbc.M609228200
- Whitaker, J. R. (1963). Determination of molecular weights of proteins by gel filtration of sephadex. *Anal. Chem.* 35, 1950–1953. doi: 10.1021/ac60205a048
- Zhou, Y., Smith, D., Leong, B. J., Brannstrom, K., Almqvist, F., and Chapman, M. R. (2012). Promiscuous cross-seeding between bacterial amyloids promotes interspecies biofilms. *J. Biol. Chem.* 287, 35092–35103. doi: 10.1074/jbc.M112.383737
- Zhou, Y., Smith, D. R., Hufnagel, D. A., and Chapman, M. R. (2013). Experimental manipulation of the microbial functional amyloid called curli. *Methods Mol. Biol.* 966, 53–75. doi: 10.1007/978-1-62703-245-2_4

Conflict of Interest: The authors declare that the research was conducted in the absence of any commercial or financial relationships that could be construed as a potential conflict of interest.

Copyright © 2020 Balistreri, Kahana, Janakiraman and Chapman. This is an open-access article distributed under the terms of the Creative Commons Attribution License (CC BY). The use, distribution or reproduction in other forums is permitted, provided the original author(s) and the copyright owner(s) are credited and that the original publication in this journal is cited, in accordance with accepted academic practice. No use, distribution or reproduction is permitted which does not comply with these terms.